SAR IMAGE SEGMENTATION THROUGH B-SPLINE DEFORMABLE CONTOURS AND FRACTAL DIMENSION

J. Gambini [*], M. Mejail [*], J. Jacobo-Berlles [*], C. Delrieux [**]

[*] Universidad de Buenos Aires, FCEyN, Departamento de Computación
Ciudad Universitaria, Pab. I, 1428 Buenos Aires, República Argentina
Tel/FAX: +54 11 4576-3359, e-mail: {jgambini, marta, jacobo}@dc.uba.ar

[**] Universidad Nacional del Sur, Departamento de Ingeniería Eléctrica
Bahía Blanca, República Argentina Tel. and FAX: ++54 291 4595154
e-mail: claudio@acm.org

Working Group WG III/4

KEY WORDS: change detection, classification, edge extraction, feature segmentation, SAR imagery

ABSTRACT

Synthetic Aperture Radar (SAR) images are usually corrupted by a signal-dependent non-additive noise called speckle. This makes difficult the segmentation, object identification, and feature extraction within this kind of images. In this work we propose the combination of local fractal estimation and B-Spline based active contours as a solution for the boundary extraction problem in SAR images. After a supervised initialization (the specification of a an initial curve laying completely within the region of interest), the algorithm searches the control points (vertices) of a B-Spline curve that fits the boundary of the region to be segmented. The vertices of the curve are found by a local estimation of the fractal dimension in the surrounding. Fractal dimension provides a good local roughens and statistical correlation estimation. Box-counting measurement of the fractal dimension is widely acknowledged to be the most adequate in terms of robustness and computational requirements. Box counting algorithms are based on a statistical analysis of the brightness distribution of the pixels in a surrounding of varying sizes. A power law can be established between the surrounding size and the amount of pixels with a given brightness profile, and then an adequate assessment of the local fractal dimension can be performed. The proposed algorithm is systematically tested on synthetic and real SAR images, and both the accuracy and the performance of our proposal are assessed.

1 INTRODUCTION

Segmentation of region boundaries is an important issue in remote sensing image analysis and many techniques have been studied to solve this problem. In the particular case of region boundary determination in SAR images, the use of Active Contours has been developed by O. Germain *et al.* (Germain, 2001), J. Jacobo *et al.* (Jacobo-Berlles et al., 2002) and M. J. Gambini *et al.* (Gambini et al., 2004) in all cases with a statistical approach.

The technique proposed in this work is based on B-Spline boundary fitting and was originally developed by A. Blake *et al.* (Blake and Isard, 1998). Blake's proposal cannot be successfully applied to SAR images due to the speckle noise, since local brightness fluctuations induce spurious control points, and therefore a bad boundary segmentation. Here, we adapt the active contours idea, but the control points are chosen in places where a local gradient in the fractal dimension are found. The boundary extraction process we describe here, begins with the application of local fractal dimension (box counting). Histogram classification of this attribute of the image allows an adequate threshold detection. Then, the determination of zones of interest, each of them includes one region for which we are going to extract the corresponding boundary. These zones of interest are given by B-Spline curves, determined by their control points. Then, a series of segments is drawn on the image, and the image data lying on them are extracted. For each segment, the transition point, that is, the point belonging to the region's boundary, is determined. This determination is based on the estimated values for the fractal dimension. Then, for each region, the contour sought is given by the B-spline curve that fits these transition points.

The structure of this paper is as follows: section 2 describes the model used here for fractal dimension estimation, section 3 gives an introduction to B-Spline curve fitting, section 4 specifies the criterion used to determine the transition points and explains the region fitting algorithm, section 5 shows the obtained results and finally, section 6 presents the conclusion an further research .

2 FRACTAL ANALYSIS FOR IMAGE SEGMENTATION

Fractal dimension analysis has been largely used as an image descriptor for segmentation. The strategies that we present here seem to produce better results in autonomous classification problems that had not been addressed before. A local image estimator that can be useful when coping with noisy images is the *fractal dimension* (Mandelbrot,

1983). The underlying idea is that random brightness distributions posses self-similar characteristics that are analogous to those of classical fractal sets (Cantor set, Sierpinsky gasket, and so on). However, self-similarity measurements cannot be applied in a strict sense since a random distribution is by definition not algorithmic. However, the relation between random distributions and fractals is very significant (Peitgen and Saupe, 1986, Mandelbrot and van Ness, 1968). The *box-counting* dimension is perhaps the best trade off between accuracy and computational complexity. In most cases this fractal dimension estimator coincides with self-similarity measurements, and even though an absolute measurement may be inaccurate, our interest in feature segmentation by relative comparison of fractal dimension is not compromised.

Box-counting dimension is based on counting the pixels visited by the set under measurement in a grid of varying resolution and position. (This assumes a previously binarized image under an adequate criterion.) Let s be the size of the side of a square cell in the grid, and $N(s)$ the average of the cells visited by the set under measurement under different translations. Then it is expected that increasing the resolution of the grid (which in fact decreases the side s of the cells of the grid in a fixed size image), $N(s)$ should also increase. The slope of this relation in logarithmic space is the *box-counting dimension* of the set:

$$D = \lim_{s \to 0} \frac{\log(N(s))}{\log(\frac{1}{s})}. \quad (1)$$

Accurate estimations should show a value of D that is stable and steady along several orders of magnitude. In experimental settings this is obviously impossible to grant, and therefore the values of D are taken as provisory.

Starting with this schema, we can find local estimators that are adequate for image segmentation. The idea is to adapt the box-counting dimension to a local context, in which only a sub-image centered around a given pixel is considered. Larger sub-images produce better measurements, but also with higher computational cost. In this work we used a grid of 5×5 pixels centered around the pixel under estimation, which showed experimentally to be a good compromise. Consider for instance the synthetic image, under a statistical model, with three different areas and a background which was generated simulating speckle noise in Figure 1(a) and its brightness histogram (Figure 1(b)). Any segmentation produced by simple binarization will be of little use. In Figure 1(c) we show a binarization under bayesian classification (marked with a circle in Figure 1(b)). However, the box-counting dimension performed on the image is remarkably good for contour extraction (see Figure 1(d)).

3 B-SPLINE REPRESENTATION

A brief theoretical review of B-spline representation of contours is presented; for more details see (Blake and Isard, 1998, Rogers and Adams, 1990).

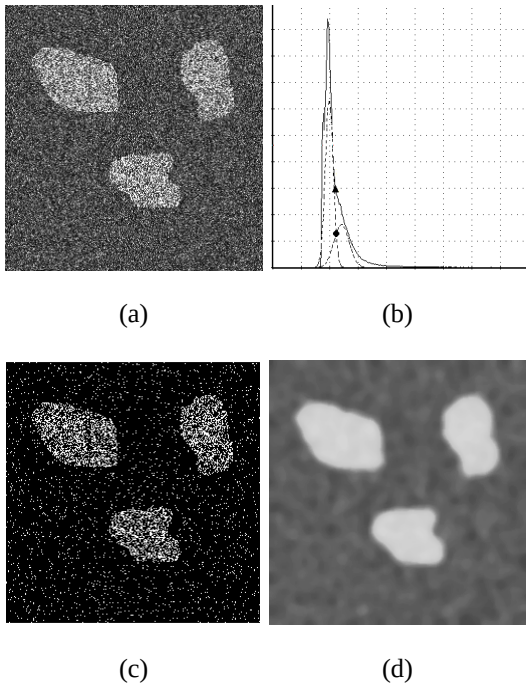

Figure 1: (a) Synthetic image under a statistical model with three different areas and a background which was generated simulating speckle noise. (b) Its brightness histogram. (c) Binarization under bayesian classification. (d) The box-counting dimension.

Let $\{Q_0, ..., Q_{N_B-1}\}$ be a set of control points, where $Q_n = (x_n, y_n)^t \in \mathbb{R}^2$, $0 \leq n \leq N_B - 1$, and let $\{s_0 < s_1 < s_2 < \cdots < s_{L-1}\} \subset \mathbb{R}$ be a set of L knots. A B-spline curve of order d is defined as a weighted sum of N_B polynomial basis functions $\mathrm{B}_{n,d}(s)$ of degree $d-1$, within each interval $[s_i, s_{i+1}]$ with $0 \leq i \leq L-1$. The constructed spline function is $r(s) = (x(s), y(s))^t$, $0 \leq s \leq L-1$, being

$$r(s) = \sum_{n=0}^{N_B-1} \mathrm{B}_{n,d}(s) Q_n,$$

and

$$x(s) = \mathrm{B}^t(s).Q^x \quad (2)$$

$$y(s) = \mathrm{B}^t(s).Q^y \quad (3)$$

where the basis functions vector $\mathrm{B}(s)$ of N_B components is given by $\mathrm{B}(s) = (\mathrm{B}_{0,d}(s), \ldots, \mathrm{B}_{N_B-1,d}(s))^t$. The weight vectors Q^x and Q^y give the first and second components of the Q_n, respectively.

The curves used in this work are closed of order $d = 3$ or $d = 4$ specified by periodic B-spline basis functions.

3.1 B-spline curve fit

The problem of determining a polygon that generates a fitting B-spline curve with known number of control points, N_B, was studied by (Rogers and Adams, 1990). We now present a brief review of this subject.

A set of k data points in the image plane is given by $\{D_0, D_1, \ldots, D_{k-1}\}$ where $D_i = (x_i, y_i)^t$, $i = 0, \ldots, k-1$, and the spline

curve that best-fits them is sought. Then, by equations 2 and 3, the components D_i must satisfy

$$x_i = \mathrm{B}^t(t_i)Q^x,$$
$$y_i = \mathrm{B}^t(t_i)Q^y,$$

for certain values of t_i, where $i = 0, \ldots, k-1$, and $N_B \leq k$.

This linear system is more compactly written in matrix form as $D = K(Q^x \quad Q^y)$, where the $k \times N_B$ elements of the real matrix K are given by $K_{ij} = B_{j,d}(t_i)$, with $i = 0, \ldots, k-1$, $j = 0, \ldots, N_B-1$, and $D = (D_0, D_1, \ldots, D_k)^t$. In the most general case $N_B < k$ and, therefore, K is not a square matrix. In this case, the pseudo-inverse matrix form $(Q^x \quad Q^y) = K^+D$ is used to find the B-spline fitting curve. A useful set of values for the parameters $\{t_0, \ldots, t_{k-1}\}$ is given by

$$t_0 = 0, \; ; t_\ell = \frac{\sum_{i=1}^{\ell} \|D_i - D_{i-1}\|}{\sum_{i=1}^{k-1} \|D_i - D_{i-1}\|}, \ell \geq 1.$$

The knot set to build the B-spline basis functions is arbitrarily chosen.

4 BOUNDARY DETECTION

In this section we describe the algorithms developed for boundary detection once the noise was removed.

4.1 Radial lines algorithms for boundary detection

Let E be a scene made up by the background B and a set of regions $\{R_1, R_2, \ldots, R_k\}$ with their respective boundaries $\{\partial R_1, ..., \partial R_k\}$. For each region R_j, we want to find the curve C_j that fits boundary ∂R_j in the image. In the first step a box-counting fractal dimension estimation is applied in order to remove the noise. We define an initial search area, which are specified by polygons, the vertexes of which are control points that generate a B-spline curve, as shown on Figure 2 with a thin line. Once the initial search zones are determined the centroid of each of them is calculated.

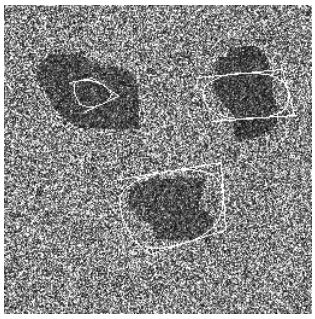

Figure 2: Initial areas of interest determinated by polygons, the vertexes of which are control points that generate a B-spline curve .

If a point belongs to the object boundary, then a sample taken from the neighborhood of that point exhibits a change in the intensity level of the box-counting image and it is considered to be a transition point. Then N segments $s^{(i)}$, $i \in \{1, ..., N\}$ with the form $s^{(i)} = \overline{CP_i}$ are considered. Here C is the centroid of the initial region, the extreme P_i is a point outside of the region and $\theta = ang\left(s^{(i)}, s^{(i+1)}\right)$ $\forall i$ is the angle between two consecutive segments, as shown on Figure 3.

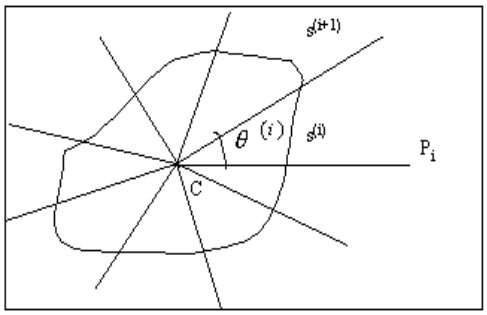

Figure 3: Radial straight lines $s^{(i)}, i = 1, ..., N$ projected from the centroid C of an initial curve to the external part of the region. $\theta^{(i)}$ is the angle between $s^{(i)}$ and $s^{(i+1)}, i = 1, ..., N-1$.

The segment $s^{(i)}$ is an array of m elements coming from a discretization of the straight line on the image. The border point b_i is found convolving the data of the segment with a mask given by $[-2, -1, 0, 1, 2]$. After find $\{b_1, ..., b_N\}$, the algorithm build the B-spline curve interpolating the border points.

4.2 Possible Problems

This algorithm gives very good results when it is applied to convex objects, but there are some situations where this method could fail. For example, it is possible that some point on the object boundary be obstructed by other point of the same boundary, so the radial straight lines will not reach this point, making it impossible to find it, as shown on Figure 4.

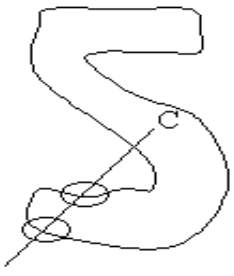

Figure 4: A non convex object. The procedure fails on the straight line segment shown on this figure. It will not detect the border points marked with a circle.

In order to solve these problems we have modified the algorithm, using an estimation of the curves's derivative at step n to predict the center of the segment $s^{(n+1)}$ at step $n+1$. This modified version calculates the velocity vector between two given boundary points b_i and b_{i+1} in the

following way:

$$\overrightarrow{v}_i = \frac{b_{i+1} - b_i}{\|b_{i+1} - b_i\|} \quad (4)$$

then, locates the segment orthogonal to the straight line direction $\overrightarrow{v}_i$, and centers it at $\lambda\overrightarrow{v}_i$, where λ is an arbitrary value. The method finds the border point b_{i+2} using the convolution with a mask, as in previous algorithm and finally build the B-spline curve interpolating the found points $\{b_1, ..., b_N\}$. The two first initial points b_1 and b_2 are found as in previous algorithm.

5 RESULTS

A synthetic image, under a statistical model, with three different city-like areas and a background with was generated simulating speckle noise. On Figure 5, the result of applying the radial straight line algorithm in a synthetic image is shown. The result of applying the algorithm which uses the velocity vector to find the contour of the interested object in a synthetic image is shown in Figure 6. This image has two regions: the object and the background. The thin line is the initial curve and the thick line is the fitting curve found by the algorithm. As it is illustrated, the method tolerates a very bad initialization step. Figure 7 (a) shows a single look real SAR image where the algorithm was applied. On Figure 7 (b), the curves result applied to the original image, is shown.

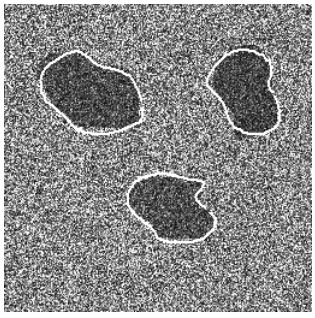

Figure 5: Result of applying the algorithm of radial lines to a synthetic image.

6 CONCLUSIONS

In this paper, a new approach to segmentation in SAR images using a classification technique based on fractal dimension and B-spline deformable contours, is described. We have shown here the boundaries of several regions which were obtained using different methods according to the features of the object. In the first step the estimated fractal dimension classification is applied to remove the noise. The second step is to find regions of interest, in a supervised manner, for each region, their respective boundaries are considered as the initial solution for the border detector. Then, a process of boundary detection is applied only

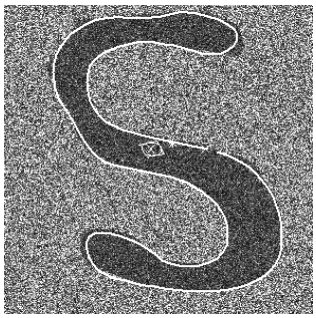

Figure 6: Result of applying the velocity algorithm to boundary extraction in a synthetic image. The thin line is the initial curve and the thick line is the fitting curve found by the algorithm. As it is illustrated, the method tolerates a very bad initialization step.

Figure 7: Result of applying the algorithm to a real SAR image.

for the data that are on a set of line segments. All these processes diminish the computational cost and improve the performance of the method. For each region, the result of the application of this algorithm is a boundary curve given by a mathematical formula expressed in terms of B-Spline functions. The results using both simulated and real SAR images are excellent with an acceptable computational effort.

REFERENCES

Blake, A. and Isard, M., 1998. Active Contours. Springer Verlag.

Gambini, M. J., Mejail, M., Jacobo-Berlles, J. C., Muller, H. and Frery, A. C., 2004. Automatic contour detection in sar images. In: Proceedings EUSAR04.

Germain, O., 2001. Edge detection and localization in SAR images: a comparative study of global filtering and active contour approaches. PhD thesis, Université de Droit, d´Economie et des Science d´Aix-Marseille.

Jacobo-Berlles, J., Gambini, M. J., Mejail, M. E., Muller, H. and Frery, A. C., 2002. Bspline curve fitting in sar images. In: Proceedings EUSAR02.

Mandelbrot, B., 1983. The Fractal Geometry of Nature. W. H. Freeman.

Mandelbrot, B. and van Ness, J., 1968. Fractional brownian motion, fractional noises and applications. Siam Review 10, pp. 422–437.

Peitgen, H. O. and Saupe, D., 1986. The Science of Fractal Images. Springer-Verlag.

Rogers, D. F. and Adams, J. A., 1990. Mathematical Elements for Computer Graphics. 2 edn, McGraw-Hill, New York, USA.